- Running head of the title: Melatonin alleviates NaF-induced hepatotoxicity
- Title: SIRT3-dependent mitochondrial oxidative stress in sodium fluoride-induced
- 3 hepatotoxicity and salvage by melatonin
- 4 **Authors:** Chao Song^{a, b, 1}, Jiamin Zhao^{a, b, 1}, Jingcheng Zhang^{a, b}, Tingchao Mao^{a, b},
- 5 Beibei Fu^{a, b}, Haibo Wu^{a, b,*}, Yong Zhang a, b,*
- Author affiliations: ^aCollege of Veterinary Medicine, Northwest A&F University,
- 7 Yangling 712100, Shaanxi, China.
- ^bKey Laboratory of Animal Biotechnology, Ministry of Agriculture, Northwest
- 9 A&F University, Yangling 712100, Shaanxi, China.
- ¹These authors contributed equally to this study.
- 11 Corresponding author: *Correspondence should be addressed to Haibo Wu or
- 12 Yong Zhang.

21

22

23

24

25

26

27

28

29

- 13 Tel.: +86 29 87080092
- 14 Fax: +86 29 87080092
- E-mail: hbwu029@nwsuaf.edu.cn (H.W) or zhangy1956@sina.com (Y.Z)
- This work was funded by the State Key Program (No. 31530075) of National
- 17 Natural Science Foundation of China and China Postdoctoral Science Foundation
- 18 Grant (No. 2016M590978)
- 19 **Keywords:** Melatonin; Sodium fluoride; Hepatotoxicity; SIRT3; PGC-1α

31

32

33

34

35

36

37

38

39

40

41

42

43

44

45

46

47

48

49

50

51

52

53

54

55

56

57

58

Abstract: Oxidative stress induced by fluoride (F) is associated with fluorosis formation, but the underlying molecular mechanism remains unclear. In this study, Melatonin pretreatment suppressed F-induced hepatocyte injury in HepG2 cells. Melatonin increases the activity of superoxide dismutase (SOD2) by enhancing sirtuin 3 (SIRT3)-mediated deacetylation and promotes SOD2 gene expression via SIRT3-regulated DNA-binding activity of forkhead box O3 (FoxO3a), indicating that melatonin markedly enhanced mROS scavenging in F-exposed HepG2 cells. Notably, melatonin activated the peroxisome proliferator-activated receptor gamma coactivator 1α (PGC- 1α). PGC- 1α interacted with the estrogen-related receptor alpha (ERRα) bound to the SIRT3 promoter, where it functions as a transcription factor to regulate SIRT3 expression. Furthermore, daily injection of melatonin for 30 days inhibited F-induced oxidative stress in mice liver, leading to improvement of liver function. Mechanistic study revealed that the protective effects of melatonin were associated with down-regulation of JNK1/2 phosphorylation in vitro and in vivo. Collectively, our data suggest a novel role of melatonin in preventing F-induced oxidative stress through activation of the SIRT3 pathway. Introduction Environmental fluoride (F) is a toxic reagent that can affect human health in various ways (Taghipour et al., 2016). Small amounts of F can be used for strengthen bones and prevention of dentals, but excessive F exposure causes a variety of pathological changes in different cells and tissues (Fu et al., 2014). The increasing F concentration in the environment combined with the intervention of human activities is cause for great concern (Ameeramja et al., 2016). The liver is the largest internal organ and the main target of F in the body. Epidemiological and clinical data have shown that excessive sodium fluoride (NaF) exposure results in liver damage (Chattopadhyay et al., 2011). As the cellular outcome of mitochondrial dysfunction, oxidative stress is strongly implicated as one of the most important mechanisms contributing to the toxic effects of NaF (Varol and Varol, 2012). Evidence suggests that the liver is highly vulnerable to oxidative stress because of

65

66

77

87

the accumulation of mitochondrial superoxide anion (O₂*-) (Mahaboob Basha and 60 Saumya, 2013). As the main mitochondrial deacetylase, sirtuin-3 (SIRT3) modulates various 61 proteins to control mitochondrial function and mitochondrial reactive oxygen 62 species (mROS) (Pi et al., 2015; Sundaresan et al., 2009). Mitochondrial manganese 63 superoxide dismutase (SOD2) is the main enzyme responsible for scavenging 64 harmful O₂ and is a substrate of SIRT3 (Kim et al., 2016; Miar et al., 2015). The binding of SIRT3 with SOD2 causes the deacetylation and activation of SOD2 (Tao et al., 2010). Moreover, SIRT3 can also interact with forkhead box O3a (FoxO3a) to 67 activate the FoxO3a-dependent antioxidant-encoding gene SOD2 (Padmaja Divya 68 69 et al., 2015). 70 Melatonin and its metabolites are powerful antioxidants and free radical scavengers (Ramis et al., 2015; Siu et al., 2006). Furthermore, melatonin modulates 71 72 mitochondrial function and strengthens its antioxidant defense systems (Dragicevic 73 et al., 2011). These effects are facilitated by its amphiphilic nature, thereby enabling melatonin to penetrate all morphophysiological barriers and enter all subcellular 74 75 compartments (Venegas et al., 2012). Recent studies have focused on the role of 76 melatonin in the regulation of mROS levels in healthy and disease states (Acuna Castroviejo et al., 2002). However, the mechanism by which melatonin protects 78 against NaF-induced hepatic oxidative injury remains obscure. 79 The data presented in the current report are the first to indicate that melatonin 80 efficiently protected against NaF-induced mitochondria-derived and O₂*-dependent 81 oxidative stress in vivo and in vitro. All these results contribute to the future clinical treatments of F-induced hepatotoxicity. 82 83 Results Melatonin attenuated F-induced oxidative injury in HepG2 cells via SIRT3 84 85 pathway Firstly, we explored the effects of melatonin on F-induced hepatotoxicity in vitro. 86 As shown in Fig. 1A, F decreased cell viability in a time- and dose-dependent

manner in HepG2 cells. However, melatonin pretreatment significantly attenuated 88 89 the adverse effect of F on cell viability (Fig. 1B). F treatment resulted in significantly elevated levels of MDA, which was attenuated by melatonin (Fig. 1C). 90 Pre-treatment with melatonin followed by F resulted in restoration of GSH (Fig. 91 92 1D). As shown in Figs 1E and F, melatonin protected the HepG2 cells against apoptosis. The expression of Bax was increased significantly in the cytosolic 93 94 fraction but decreased significantly in the mitochondrial fraction in HepG2 cells 95 when treated with F. The Bax/Bcl-2 ratio after F treatment increased in the cytosolic fraction but significantly decreased in the mitochondrial fraction of HepG2 cells. 96 By contrast, melatonin pretreatment inhibited F-induced changes of Bax/Bcl-2 ratio 97 in the cytosolic and mitochondrial fractions. 98 As the main mitochondrial deacetylase, sirtuin-3 (SIRT3) modulates various 99 proteins to control oxidative stress response. Melatonin pretreatment significantly 100 101 recovered the reduced SIRT3 expression (Fig. 2A) and activity (Fig. 2B), which 102 was induced by F. Loss of SIRT3 diminished the effects of melatonin-induced the 103 up-regulated expression and activity of SIRT3. We found that melatonin could protect against F-induced mitochondria-derived O₂•- elevation (Fig. 2C) and cell 104 105 viability reduction (Fig. 2D). As shown in Fig. 2E, melatonin significantly blocked 106 the increase in apoptosis induced by F. Furthermore, melatonin treatment inhibited 107 the collapse of MMP induced by F (Fig. 2F). However, these beneficial effects of 108 melatonin were significantly attenuated by SIRT3 siRNA transfection. These data 109 suggest a SIRT3-dependent effect of melatonin on oxidative stress response in 110 hepatic cells exposed to F. Moreover, HepG2 cells were also incubated with F in the presence of Mito-TEMPO 111 112 (mitochondria-targeted SOD mimetic). Treatment with Mito-TEMPO significantly 113 enhanced SOD2 activity but not SOD2 protein levels (Figs. S1A and B). The F-induced increase in oxidative injury was significantly attenuated in the presence 114 115 of Mito-TEMPO (Figs. S1c-e). 116 .Melatonin inhibits mitochondria-derived O₂ - accumulation via SOD2

118

119

120

121

122

123

124

125

126

127

128

129

130

131

132

133

134

135

136

137

138

139

140

141

142

143

144

145

upregulation in HepG2 cells SOD2 is a mitochondrial antioxidant that aids in the elimination of $O_2^{\bullet-}$. As shown in Figs. 3A and B, loss of SIRT3 diminished the effects of melatonin-induced the up-regulated expression and activity of SOD2. SIRT3-mediated deacetylation of SOD2 and the subsequent regulates its antioxidant activity, we further studied the relationship between the influence of melatonin on SOD2 activity and SIRT3. Coimmunoprecipitation pull-down (Co-IP) assay results indicated that melatonin promoted the binding of SOD2 and SIRT3 in mitochondria under F exposure (Fig. 3C), and caused the decreased acetylation of SOD2 (Fig. 3D). SIRT3 knockdown diminished the effects of melatonin on the acetylation levels of SOD2 (Fig. 3E). Overexpression of SIRT3 significantly rescued F-induced suppression of SIRT3 expression (Fig. 4A) and activity (Fig. 4B). Moreover, overexpression of SIRT3, but not SIRT3^{H248Y} (a catalytic mutant of SIRT3 lacking deacetylase activity), decreased the expression of acetylated-SOD2 and increased SOD2 activity in HepG2 cells exposed to NaF (Figs. 4C and D). The deacetylase-deficient Sirt3 mutant (H248Y) completely eliminated the protective effects of SIRT3 (Figs. 4E and F). These results indicate that the deacetylation of SOD2 induced by melatonin is mediated by SIRT3 and melatonin enhances SOD2 activity through the deacetylation of SIRT3. Melatonin increased SOD2 expression via the interaction of SIRT3 with FoxO3a. As shown in Fig. 5A, melatonin pretreatment had little influence on the total protein level of FoxO3a in F-treated HepG2 cells. Treatment of HepG2 cells with F caused increased the phosphorylation of FoxO3a at serine 253 (Fig. 5B) and the acetylation of FoxO3a at the K-100 lysine (Fig. 5C). Both events prevented nuclear import, thereby leading to its inactivation. Melatonin pretreatment decreased the phosphorylation at Ser253 and comparably increased FoxO3a deacetylation. Loss of SIRT3 diminished the effects of melatonin on the deacetylation and phosphorylation of FoxO3a. SIRT3 and FoxO3a functionally and physically interact

147

148

149

150

151

152

153

154

155

156

157

158

159

160

161

162

163

164

165

166

167

168

169

170

171

172

173

174

to form a complex that regulates the activity and acetylation status of FoxO3a. Our results showed that melatonin promoted the interaction of FoxO3a with SIRT3 in mitochondria (Fig. 5D). Moreover, the FoxO3a-luciferase reporter gene assay indicated that melatonin increased the transcriptional activity of FoxO3a. When the cells were co-transfected with the pGL-FHRE-luc plasmid and SIRT3 siRNA, the regulative activities of melatonin were abolished (Fig. 5E). The ChIP assay was then performed to investigate the role of FoxO3a in the melatonin-induced SOD2 expression of FoxO3a. In the ChIP assay, melatonin promoted the binding of FoxO3a to the promoter of SOD2 (Fig. 5F) under F exposure. The manipulation of SIRT3 expression, but not that of SIRT3^{H248Y}, restored activation of FoxO3a by decreasing phosphorylation at Ser253 (Figs. 6A and B) and comparably increasing FoxO3a deacetylation (Fig. 6C). Overexpression of SIRT3 increased the transcriptional activity of FoxO3a (Fig. 6D) and restored the F-induced reduction FoxO3a binding to the gene promoter of SOD2 (Fig. 6E). Melatonin activated the PGC-1α/ERRα-SIRT3 signaling pathway in HepG2 cells Next, we sought to determine which factor mediates the expression of SIRT3. As shown in Figure. 7A, SIRT3 expression was regulated at the transcription level. SIRT3 was previously reported to be regulated by PGC-1a. So we examined PGC-1a expression with western blotting and found that PGC-1a was changed with a similar change pattern of SIRT3 expression (Fig.2B). PGC-1α siRNA transfection prevented the induction of SIRT3 expression in HepG2 cells, thereby indicating that PGC-1α was required for the activation of melatonin during SIRT3 expression. Since ERR α acts as the downstream target of PGC-1 α and is co-activated by this transcriptional coactivator. Here we found that PGC-1α interacted with ERRα in HepG2 cells (Fig. S2A). Knockdown of ERRα or PGC-1α decreased SIRT3 expression and cotransfection of ERRα siRNA and PGC-1a siRNA could decrease more expression of SIRT3 (Fig. S2B), while overexpression of PGC-1α or ERRα increased SIRT3 expression and cotransfection of PGC-1 α and ERR α could

176

177

178

179

180

181

182

183

184

185

186

187

188

189

190

191

192

193

194

195

196

197

198

199

200

201

202

203

increase more expression of SIRT3 (Fig. S2C). These results indicate that PGC-1a and $ERR\alpha$ coordinately regulate SIRT3 expression in HepG2 cells. Furthermore, the luciferase assay was used to determine if SIRT3 mRNA activation by melatonin occurred via PGC-1α-dependent ERRα binding to the SIRT3 promoter. As shown in Fig. 7C, F exposure caused a significant decrease in the luciferase activity as compared with the control group. By contrast, melatonin pretreatment significantly increased the ERRE-mediated SIRT3 transcriptional activity, whereas this effect was diminished by the addition of PGC-1 α siRNA. The EMSA assay was further performed to test the *in vitro* binding of ERRα and SIRT3 fragments. A preliminary experiment was performed to test the binding of probe (Fig. 7D-1). As shown in Fig. 7D-2, a band in the lane loaded with WT probe and lysates was shifted as compared with lysates alone. The protein-probe binding was regulated by F and melatonin. Moreover, a specific super-shift band was detected with the ERR α antibody, thereby indicating that ERR α was bound to the probe (Fig. 7D-3). The results of EMSA also showed that melatonin increased the binding of the exogenous consensus DNA oligonucleotide of SIRT3 with ERRα. To further confirm the EMSA results and verify that ERRα physically occupies the SIRT3 promoter, we performed the ChIP assay. As shown in Fig. 7E, a 3.6-fold enrichment of ERRa was observed. Melatonin attenuated F-induced JNK1/2 activation in mice liver Furthermore, we also investigate whether melatonin could prevent F-induced oxidative stress in mice liver. Significant accumulation of F was observed in F-toxicated mice liver (Fig. S3A). Liver functions were also measured based on changes in the hepatic markers ALT and AST. The results showed that the serum activities of ALT and AST were significantly increased in the F group when compared with the control group (Figs. S3B and C). This result confirmed that F-toxicity model had been successfully established. Melatonin supplementation caused a significant reduction in the accumulated F-content and the serum activities of ALT and AST. Moreover, Melatonin treatment successfully attenuated the

205

206

207

208

209

210

211

212

213

214

215

216

217

218

219

220

221

222

223

224

225

226

227

228

229

230

231

232

F-induced upregulation of O₂*- and MDA content (Figs. S3D and E). Moreover, GSH level were decreased significantly in F-toxicated mice livers, which was reversed by melatonin (Fig. S3F). Since apoptosis plays an important role in the pathogenetic mechanisms involved in fluorosis. NaF treatment increased caspase-3 activity (Fig. 8A), an indicator of apoptosis, and decreased the protein levels of Bcl-2 (Fig. 8B), an important anti-apoptotic factor in mice liver. Pretreatment with melatonin attenuated caspase-3 activity and increased Bcl-2 protein expression in NaF-treated mice liver. Activation of mitogen-activated protein kinase (MAPK) has been implicated in F-induced apoptosis and they are sensitive to oxidative stress, Western blot showed that the melatonin significantly reduced the phosphorylation of JNK1/2 in F-exposed mice liver. To further address the involvement of JNK1/2, HepG2 cells were pretreated melatonin or SP600125 (a potent JNK1/2 inhibitor). Our results showed that F-induced JNK1/2 activation in HepG2 cells, which was significantly reduced by melatonin or SP600125 (Fig. 8C). In addition, caspase-3 activity were reduced in F-treated HepG2 cells following pretreatment with melatonin or JNK inhibitor (Fig. 8D). **DISCUSSION** Oxidative stress from excessive mROS plays an important role in the pathogenesis of F-mediated cytotoxicity (Chouhan and Flora, 2008; Gao et al., 2008). SOD2 is crucial for maintaining the mitochondria-derived O₂ balance (Li et al., 2004). In the present study, SOD2 expression and activity were significantly reduced in NaF-treated HepG2 cells. Pretreatment with melatonin promotes SOD2 activity and expression, thereby protecting liver cells from mROS induced oxidative stress under excessive F exposure. Moreover, treatment with the mitochondria-targeted antioxidant Mito-TEMPO alleviated cellular oxidative stress and increased cell viability. The maintenance of mitochondria-derived O₂• at tolerable levels may be a viable strategy to treat F-induced cellular damage.

234

235

236

237

238

239

240

241

242

243

244

245

246

247

248

249

250

251

252

253

254

255

256

257

258

259

260

261

Oxidative stress is the cellular outcome of mitochondrial dysfunction. The MMP is a measure of mitochondrial function (Gong et al., 2014). The diminished membrane potential in the present study is consistent with previous findings in fluorosis (Yan et al., 2015). Moreover, mitochondrial dysfunction was further aggravated by the down regulation of SOD2 which is critical for maintaining mitochondrial oxidative balance. As the primary mitochondrial deacetylase, SIRT3 regulates the biological functions directly involved in mitochondrial function and oxidative stress response (Ansari et al., 2016; Qiu et al., 2010). SIRT3 also has a positive role in maintaining the MMP (Zhou et al., 2014). Melatonin treatment ameliorates mitochondrial oxidative stress by scavenging for enhanced mROS and improving the mitochondrial function. SOD2 is a substrate of SIRT3 in mitochondria; the binding of SIRT3 with SOD2 causes SOD2 deacetylation, thereby enhancing the mitochondrial scavenging capacity (Chen et al., 2011; Qiu et al., 2010). Our current findings indicate that melatonin promotes SOD2 deacetylation in mitochondria, which was suppressed by SIRT3 siRNA transfection. Furthermore, a catalytic mutant of SIRT3 (SIRT3^{H248Y}). which lacks deacetylase activity, failed to reverse the F-induced increase in mitochondria-derived O₂. Therefore, SIRT3 activates SOD2 via its deacetylase activity to inhibit O₂ - accumulation. SIRT3 directly targets SOD2 and promotes SOD2 transcription by FoxO3a activation, thereby protecting cells from cellular oxidative stress (Du et al., 2013; Wei et al., 2015). Nuclear localization of FoxO3a is essential for its transcriptional activity and the transcription of FoxO3a-dependent genes (Calnan and Brunet, 2008; Tseng et al., 2013). In the present study, F treatment increased FoxO3a phosphorylation at Ser253, thereby inactivating FoxO3a and preventing its nuclear import to inactivate HepG2 cells. Melatonin promotes the interaction of FoxO3a with SIRT3 and enhances FoxO3a deacetylation in the mitochondria; thus the translocation of FoxO3a from mitochondria to nucleus is promoted, thereby causing its complex influence on SOD2 transcription, which controls mitochondria-derived

267

290

O₂*-. Collectively, our findings indicate that melatonin enhances SOD2 expression 262 by promoting SIRT3-regulated FoxO3a transcriptional activity under excessive F 263 264 exposure. Melatonin-induced SIRT3 activation plays a pivotal role in protecting against F-induced oxidative stress. The transcriptional coactivator PGC-1α is a crucial 266 regulator in mitochondrial biogenesis, energy generation, and oxidative stress 268 response (Houten and Auwerx, 2004; Millay and Olson, 2013). Furthermore, a 269 current study indicated that PGC-1α stimulated mouse SIRT3 activity in both 270 hepatocytes and muscle cells, indicating that PGC-1α acts as an endogenous 271 regulator of SIRT3 (Park et al., 2012). Recent work highlights the key role of 272 PGC-1α in melatonin-regulated hepatic mitochondrial health. Our study is the first 273 to reveal that melatonin activates SIRT3 mRNA transcription via a 274 PGC-1α-dependent signaling pathway. PGC-1a interacts with the SIRT3 275 transcription factor ERRa as a transcriptional coactivator for the expression of 276 SIRT3 in F-induced liver cells injury. 277 Oxidative stress have been demonstrated to activate a variety of signaling pathways, 278 among which ERK1/2 and JNK1/2 have been implicated in F-induced apoptosis 279 (Geng et al., 2014). Here, melatonin pretreatment prevented JNK1/2 activation induced by F in vivo and in vitro. Inhibition of JNK1/2 prevented F-induced 280 281 apoptosis. Thus, blocking JNK1/2 signaling may represent a potential mechanism 282 underlying the protection of melatonin. 283 In summary, we obtained evidence for the first time to demonstrate mROS 284 inhibition by melatonin reduces F-induced oxidative stress via SIRT3 upregulation 285 in HepG2 cells. Melatonin enhances SOD2 activity by promoting SIRT3-mediated 286 deacetylation, but also increases SOD2 expression by increasing the transcriptional 287 activity of FoxO3a. Our results further highlight the potential importance of melatonin in SIRT3-mediated mROS homeostasis, thereby illustrating a novel 288 289 molecular mechanism of melatonin to be explored for future clinical treatment of F-induced hepatotoxicity.

291 Materials and methods **Ethics statement** 292 This study was performed in strict accordance with the guidelines for the care and 293 use of animals of Northwest A&F University. All animal experimental procedures 294 295 were approved by the Animal Care Commission of the College of Veterinary Medicine, Northwest A&F University. 296 **Chemicals and reagents** 297 All chemicals and reagents were obtained from Sigma-Aldrich Chemical Co. (St. 298 299 Louis, MO, USA) unless otherwise stated. Antibodies against Bax, Bcl-2, GAPDH, β-actin, COX IV, SOD2, SIRT3, acetylated-lysine, ERRα, and c-Jun NH2-terminal 300 301 kinase-1/2 (JNK1/2) were purchased from Cell Signaling Technology (Beverly, MA, USA). Antibodies against FoxO3a, phospho-FoxO3a (Ser 253), and PGC-1α were 302 obtained from Abcam (Cambridge, UK). 303 304 Cell culture and treatment 305 HepG2 cells were purchased from the American Type Culture Collection (ATCC, 306 Manassas, USA). The HepG2 cells were cultured in Dulbecco's Modified Eagle's Medium (DMEM, Gibco, USA), which was supplemented with 10 % 307 heat-inactivated fetal bovine serum (FBS, Gibco) in a 5 % CO₂ humidified 308 atmosphere at 37 °C. Cells were pretreated with 40 µM melatonin for 2 h, washed, 309 310 and treated with or without NaF (2 mM) for an additional 12 h. Experimental protocol are described in more details in Supporting information. 311 Cell viability 312 313 Cell viability was analyzed using Cell Counting Kit-8 (Beyotime, Jiangsu, China). The absorbance was obtained with a microplate reader (Epoch, BioTek, Luzern, 314 315 Switzerland) set at a wavelength of 450 nm. 316 Assay of biochemical makers of oxidative stress 317 The concentrations of malondialdehyde (MDA) and glutathione (GSH), and the activity of SOD2 were assayed by commercial assay kits purchased from Nanjing 318 319 Jiancheng Bioengineering Institute (Nanjing, Jiangsu, China).

320 Apoptosis analysis 321 Cell apoptosis was detected with the Annexin V-fluorescein isothiocyanate (FITC) Apoptosis Detection kit (Beyotime) and analyzed on the BD LSR II flow cytometry 322 system (Becton Dickinson, Franklin Lakes, NJ, USA). 323 Isolation of cytosolic and mitochondrial fractions 324 Mitochondrial fractions were immediately extracted with the Cytosolic and 325 326 Mitochondria Isolation Kit (Beyotime). Protein concentrations were determined 327 with the BCA Protein Assay Kit (Pierce Biotech, Rockford, IL, USA). 328 **Immunoblot analysis** Immunoblot analysis was performed as described in the protocols provided by the 329 330 primary antibody suppliers. **SIRT3** activity 331 Protein was extracted with a mild lysis buffer (50 □ mM Tris-HCl, pH 8; 125 □ mM 332 333 NaCl; $1 \square$ mM DTT; $5 \square$ mM MgCl₂; $1 \square$ mM EDTA; 10 % glycerol; 0.1% NP-40). SIRT3 activity was determined with the CycLex SIRT3 Deacetylase Fluorometric 334 Assay Kit according to the manufacturer's instructions (MBL International Corp. 335 336 Tokyo, Japan). The fluorescence intensity was monitored at excitation and emission wavelengths of 355 and 460 nm, respectively. 337 Mitochondrial O₂ - assessment 338 339 Mitochondrial O₂ generation was assessed in HepG2 cells by 10 μM MitoSOX 340 (Molecular Probes, CA, USA) for 20 min at 37 °C. The fluorescence intensity was 341 measured with an InfiniteTM M200 Microplate Reader (Tecan, Mannedorf, 342 Switzerland) at excitation and emission wavelengths of 492 and 595 nm, respectively. 343 344 **RNA** interference 345 The siRNA targeting SIRT3 and PGC-1α were purchased from Santa Cruz Biotechnology (Santa Cruz, CA, USA). Cells were transfected with the 346 347 non-targeted control siRNA to target small interfering RNAs for 6 h according to 348 the manufacture's protocol. At 24 h after transfection, cells were harvested for

further experiments. 349 Mitochondrial membrane potential (MMP) 350 MMP was detected with the fluorescent, lipophilic dye, JC-1 (BioVision, Milpitas, 351 CA, USA) as previously described (Ye et al., 2011). 352 **Immunoprecipitation (IP)** 353 354 IP was conducted according to previously described methods (Lai et al., 2013) with 355 a few modifications. Lysates were clarified by centrifugation at 14,000×g for 15 356 min and adjusted to the same protein concentration with the respective lysis buffer 357 for IP. Briefly, protein extracts were incubated overnight at 4 °C with the anti-SIRT3, SOD2 or FoxO3a antibody before fresh protein A/G-conjugated beads 358 359 (Santa Cruz) were added and rotated overnight at 4 °C. Finally, the beads were 360 washed thrice with the same lysis buffer, eluted with the sample loading buffer, and subjected to immunoblot analysis. 361 362 Plasmids and transfection 363 SIRT3 cDNA was cloned from HepG2 cells and inserted into the EcoRI/XhoI site of the vector pIRES-hrGFP-1a. The mutant of SIRT3 (H248Y) was generated with 364 the Quick Change Site-directed Mutagenesis Kit (Stratagene, Santa Clara, CA, 365 USA). Cells were washed after 24 h of transfection and processed for further 366 studies. All the primers used for plasmids construction are listed in Supporting 367 368 Information Table S1. 369 **Immunofluorescence staining** 370 Cells were fixed with 4% formaldehyde, permeabilized with 0.5% Triton X-100, 371 washed with PBS, blocked for 1 h with 10 % bovine serum albumin, and incubated with rabbit monoclonal anti-pFoxO3a (S253) overnight at 4 °C. The cells were then 372 washed and incubated with FITC- conjugated secondary antibodies (Santa Cruz) for 373 374 1 h at room temperature, and nuclei were revealed with DAPI (10 mg/ml; 375 Sigma–Aldrich Co., St. Louis, MO). The stained cells were observed by fluorescence microscopy (Nikon, Tokyo, Japan). 376 377 Luciferase reporter assay

379

380

381

382

383

384

385

386

387

388

389

390

391

392

393

394

395

396

397

398

399

400

401

402

403

404

405

406

Luciferase measurements were performed with the dual luciferase reporter (DLR) Assay System (Promega, Madison, WI, USA). pGL-FHRE-Luc (reporter plasmid for FoxO3a) and pGL-ERRE-Luc (reporter plasmid for ERRα) plasmids were obtained from Addgene (Cambridge, MA, USA). Briefly, cells were transfected with 2 µg of reporter plasmid/well and 0.1 µg of Renilla luciferase plasmid pRL-SV40 (Promega) was co-transfected as an internal control. Data were collected with a VICTOR X5 Multilabel Plate Reader (PerkinElmer). Quantitative Real-time PCR (qPCR) analysis Total RNA was isolated with the TRIzol Reagent (Invitrogen), which was reverse transcribed to cDNA with the SYBR PrimeScript RT-PCR Kit (Takara BIO Inc., Japan). The gene-specific primers used are listed in Supporting Information Table S2. Results were normalized to levels of GAPDH mRNA and expressed as the fold change $(2^{-\Delta\Delta Ct})$. Chromatin immunoprecipitation assay (ChIP) A ChIP assay was performed with the Pierce Agarose ChIP Kit as previously described (Wu et al., 2014). Briefly, cells were cross-linked with formaldehyde for 15 min at room temperature followed by glycine treatment to stop the cross-linking. Genomic DNA was isolated and sheared by ultrasonic waves and 10 % of the supernatant was regarded as input. Antibodies against FoxO3a or ERRα were used for IP. The ChIP enrichment was determined with an ABI StepOnePlus PCR system (Applied Biosystems). Primer sequences used for ChIP-qPCR are listed in Supporting Information Table S3. Electrophoretic mobility shift assay (EMSA) The EMSA assay was strictly performed with an Electrophoretic Mobility Shift Assay Kit (Molecular Probes, Invitrogen) according to the manufacturer's recommendations. Primer sequences used for EMSA are listed in Supporting Information Table S4. **Animal studies** A total of 40 two-mo-old Kunming mice were purchased from the experimental

408

409

410

411

412

413

414

415

416

417

418

419

420

421

422

423

424

425

426

427

428

429

430

431

432

433

434

435

animal center of the Fourth Military Medical University. The mice were kept in standard animal housing at 22 ± 2 °C with ventilation and hygienic conditions, as well as free access to food and water. Animals were randomly divided into four groups of 10 each. Group 1 (Control): Mice was provided distilled water and received daily injection vehicle for 30 days. Group 2 (Mel): Mice were received daily injection of melatonin alone (5 mg/kg/day, i.p.) for 30 days (San-Miguel et al., 2015). Group 3 (F): Mice were supplied with 120 mg/L NaF in deionized water and received daily injection vehicle for 30 days according to our previous study (Fu et al., 2014). Group 4 (Mel + F): Mice were administrated with 120 mg/L NaF in drinking water and received daily injection of melatonin for 30 days. After treatment, the F concentration in the liver was estimated with an ion-sensitive electrode, as previously described (Zhou et al., 2013). Values were expressed as µg F per g dry tissue. The livers were homogenized in nine fold (w/v) cold normal saline using an automatic homogenizer, and centrifuged at 1500×g for 20 min at 4 °C. The supernatant was kept at -80 °C until further analysis. **Liver function** Liver function was evaluated by measuring serum alanine aminotransferase (ALT) and aspartate aminotransferase (AST) with an automated chemistry analyzer (Olympus AU1000, Olympus, Tokyo, Japan). Statistical analysis Raw data were analyzed with the SPSS 19.0 software (Chicago, IL, USA). Results are expressed as mean \pm SD from triplicate parallel experiments unless otherwise indicated. Statistical analyses were performed with one-way ANOVA, followed by post hoc least significant difference tests. Values with P<0.05 were considered statistically significant. **Acknowledgments** This work was funded by the State Key Program (No. 31530075) of National Natural Science Foundation of China and China Postdoctoral Science Foundation

Grant (No. 2016M590978). 436 **Competing interests** 437 The authors indicate no competing financial interest. 438 439 **Author contributions** Chao Song: Conception and design, collection and assembly of data, data analysis 440 and interpretation, manuscript writing 441 442 Jiamin Zhao: Collection and assembly of data 443 Jingcheng Zhang: Collection and assembly of data 444 Tingchao Mao: Collection and assembly of data 445 Beibei Fu: Collection and assembly of data 446 Haibo Wu: Conception and design, collection and assembly of data, data analysis 447 and interpretation Yong Zhang: Conception and design, data analysis and interpretation, financial 448 449 support, final approval of manuscript 450 **Figure Legends** FIGURE 1 Melatonin inhibited NaF-induced hepatic injury in HepG2 cells. (A) 451 Cells were treated with NaF with different concentrations or for different time 452 intervals, respectively. Cell viability was determined using the CCK-8 assay. (B) 453 Confluent cells were pretreated for 2 h with various concentrations of melatonin. 454 455 After removing the supernatants, cells were incubated with fresh medium in the 456 presence or absence of NaF (2 mM) for an additional 12 h. Cell viability was 457 determined. (C) GSH level. (D) MDA content. (E) Representative images of flow 458 cytometric analysis by Annexin V-FITC/PI dual staining. (F) The ratio of 459 Bax/Bcl-2 in the cytosolic fraction and mitochondrial fraction. All results are representative of three independent experiments and values are presented as means 460 \pm SD. *p < 0.05, **p < 0.01 versus the control group, **p < 0.01 vs. the F group. 461 FIGURE 2 Melatonin protected against NaF-induced oxidative injury via 462 SIRT3 pathway. Cells were transfected with SIRT3 siRNA. At 24-h 463 464 post-transfection, cells were pretreated with melatonin (40 µM) for 2 h and then

465 treated with or without NaF of 2 mM for an additional 12 h. SOD2 expression (A) and activity (B), the mitochondrial O_2^{\bullet} levels (C), cell viability (D), apoptosis (E), 466 467 and MMP (F) were determined, respectively. The scale bar is 50 µm. All results are presented as means \pm SD of at least three independent experiments. *p < 0.05, **p < 468 0.01 versus siNC + control group, ##p < 0.01 versus the siNC + F group, \$\$p < 0.01 versus the siNC + F group,469 470 versus the siNC+Mel+F group. 471 FIGURE 3 Melatonin increased mROS scavenging by stimulating 472 **SIRT3-mediated SOD2 deacetylation.** Cells were transfected with SIRT3 siRNA. 473 At 24-h post-transfection, cells were pretreated with melatonin (40 µM) for 2 h and then treated with or without NaF of 2 mM for an additional 12 h. (A) SOD2 474 475 expression. (B) SOD2 activity. (C) SOD2 was immunoprecipitated using SIRT3 476 antibody. (D) acetylated-SOD2 (Ac-SOD2) was immunoprecipitated using SOD2 antibody. (E) Ac-SOD2 was immunoprecipitated in SIRT3-deficient HepG2 cells. 477 All results are representative of three independent experiments. **p < 0.01 versus 478 siNC + control group, ##p < 0.01 versus the siNC + F group, \$\$p < 0.01 versus the 479 siNC+Mel+F group. 480 FIGURE 4 SIRT3 deacetylase deficiency does not affect SOD2 acetylation and 481 oxidative injury in F-treated HepG2 cells. Cells were transfected with SIRT3 482 expression constructs (WT or H248Y) followed by exposure to NaF (2 mM) for 12 483 h. (A) SIRT3 expression, (B) SIRT3 activity. (C) Acetylation of SOD2 was 484 485 determined by immunoprecipitation. (D) SOD2 activity. (E) Mitochondrial-derived $O_2 \bullet^-$ production. (F) Cell viability. **p < 0.01 versus scramble + F group, *#p < 0.01 486 487 versus the SIRT3 + F group. FIGURE 5 Melatonin regulated the expression of SOD2 through the 488 interaction of SIRT3 with FoxO3a in mitochondria. (A) Mitochondria were 489 490 isolated after treatment and subjected to western blot analysis for FoxO3a. (B and C) 491 Expressions of p-FoxO3a and FoxO3a acetylation at lysine-100 residue. (D) FoxO3a was immunoprecipitated using a SIRT3 antibody. (E) Cell lysates were 492 493 harvested for dual luciferase report assays. (F) ChIP analysis was used to examine

495

496

497

498

499

500

501

502

503

504

505

506

507

508

509

510

511

512

513

514

515

516

517

518

519

520

521

522

the binding of FoxO3a to the SOD2 promoter. Data are presented as the mean \pm SD of three independent experiments. *P<0.05, **P<0.01 versus the Control group. FIGURE 6 SIRT3 deacetylase deficiency does not affect SOD2 expression and in F-treated HepG2 cells. Cells were transfected with SIRT3 expression constructs (WT or H248Y) followed by exposure to NaF (2 mM) for 12 h. (A and B) The expression of pFoxO3a, FoxO3a, and SOD2. (C) FoxO3a acetylation at lysine-100 residue was examined. (D) Cell lysates were harvested for dual luciferase report assays. (E) Binding of FoxO3a to SOD2 was examined using ChIP assay. The scale bar is 50 μ m. Data are presented as the mean \pm SD of three independent experiments. **P<0.01 versus the F + Scramble group, \$\$P<0.01 versus the F + SIRT3 group. FIGURE 7 Melatonin activated PGC-1α/ERRα-SIRT3 signaling pathway in **HepG2 cells.** Cells were transfected with PGC- 1α siRNA. At 24-h post-transfection, cells were pretreated with melatonin (40 µM) for 2 h and then treated with or without NaF of 2 mM for an additional 12 h. (A) SIRT3 mRNA level. (B) The expression of PGC-1a and SIRT3. (C) ERRα luciferase reporter plasmid was transfected into HepG2 cells. Luciferase activity was determined. (D) In vitro binding of ERRα and SIRT3 promoter was examined by EMSA assay. (E) In vivo binding of ERRα and SIRT3 promoter was examined by the ChIP assay. Data are presented as the mean \pm SD of three independent experiments. *p < 0.05, **p < 0.01 versus the siNC + control group; $^{\#}p < 0.05$, $^{\#\#}p < 0.01$ versus the siNC + F group, and p < 0.05 versus the siNC +Mel + F group. Abbreviation: WT, wild-type; MUT, mutation; Ab, antibody. FIGURE 8 Melatonin inhibited JNK1/2 activation in mice liver. (A) Caspase-3 activity (H). (B) The representative western blot for Bax, Bcl-2, JNK1/2 in mice liver. (C) Immunoblot analysis in HepG2 cells. (D) Caspase-3 activity was determined in HepG2 cells. Data are mean \pm SD; n = 6–8. *p < 0.05 or 3 different cultures., **p < 0.01 versus the control group, **p < 0.05, ***p < 0.01 versus the F group.

524

525

526

527

528

529

530

531

532

533

534

535

536

537

538

539

540

541

542

543

544

545

546

547

548

549

Abbreviations: Sodium fluoride, NaF; Melatonin, Mel; Mitochondrial reactive oxygen species, mROS; Mitochondrial manganese superoxide dismutase, SOD2; Peroxisome proliferator-activated receptor gamma coactivator 1α, PGC-1α; Estrogen-related receptor alpha, ERRα; Malondialdehyde, MDA; Glutathione, GSH; Chromatin immunoprecipitation assay, ChIP; Electrophoretic mobility shift assay, EMSA. Alanine aminotransferase, ALT; Aspartate aminotransferase, AST; d c-Jun NH2-terminal kinase-1/2, JNK1/2; WT, wild-type; MUT, mutation; Ab, antibody. References Acuna Castroviejo, D., Escames, G., Carazo, A., Leon, J., Khaldy, H. and Reiter, R. J. (2002). Melatonin, mitochondrial homeostasis and mitochondrial-related diseases. Curr Top Med Chem 2, 133-51. Ameeramja, J., Panneerselvam, L., Govindarajan, V., Jeyachandran, S., Baskaralingam, V. and Perumal, E. (2016). Tamarind seed coat ameliorates fluoride induced cytotoxicity, oxidative stress, mitochondrial dysfunction and apoptosis in A549 cells. J Hazard Mater 301, 554-65. Ansari, A., Rahman, M. S., Saha, S. K., Saikot, F. K., Deep, A. and Kim, K. **H.** (2016). Function of the SIRT3 mitochondrial deacetylase in cellular physiology, cancer, and neurodegenerative disease. Aging Cell. Calnan, D. R. and Brunet, A. (2008). The FoxO code. *Oncogene* 27, 2276-88. Chattopadhyay, A., Podder, S., Agarwal, S. and Bhattacharya, S. (2011). Fluoride-induced histopathology and synthesis of stress protein in liver and kidney of mice. Arch Toxicol **85**, 327-35. Chen, Y., Zhang, J., Lin, Y., Lei, Q., Guan, K. L., Zhao, S. and Xiong, Y. (2011). Tumour suppressor SIRT3 deacetylates and activates manganese superoxide dismutase to scavenge ROS. EMBO Rep 12, 534-41.

550 Chouhan, S. and Flora, S. J. S. (2008). Effects of fluoride on the tissue 551 oxidative stress and apoptosis in rats: Biochemical assays supported by IR 552 spectroscopy data. *Toxicology* **254**, 61-67. Dragicevic, N., Copes, N., O'Neal-Moffitt, G., Jin, J., Buzzeo, R., Mamcarz. 553 554 M., Tan, J., Cao, C., Olcese, J. M., Arendash, G. W. et al. (2011). Melatonin 555 treatment restores mitochondrial function in Alzheimer's mice: a mitochondrial 556 protective role of melatonin membrane receptor signaling. J Pineal Res 51, 75-86. 557 Du, K., Yu, Y., Zhang, D., Luo, W., Huang, H., Chen, J., Gao, J. and Huang, C. (2013). NFkappaB1 (p50) suppresses SOD2 expression by inhibiting FoxO3a 558 transactivation in a miR190/PHLPP1/Akt-dependent axis. Mol Biol Cell 24, 559 3577-83. 560 Fu, M., Wu, X., He, J., Zhang, Y. and Hua, S. (2014). Natrium fluoride 561 562 influences methylation modifications and induces apoptosis in mouse early 563 embryos. Environ Sci Technol 48, 10398-405. 564 Gao, Q., Liu, Y. J. and Guan, Z. Z. (2008). Oxidative stress might be a 565 mechanism connected with the decreased alpha 7 nicotinic receptor influenced by high-concentration of fluoride in SH-SY5Y neuroblastoma cells. Toxicol In Vitro 22, 566 567 837-43. Geng, Y., Qiu, Y., Liu, X., Chen, X., Ding, Y., Liu, S., Zhao, Y., Gao, R., 568 Wang, Y. and He, J. (2014). Sodium fluoride activates ERK and JNK via induction 569 570 of oxidative stress to promote apoptosis and impairs ovarian function in rats. J 571 Hazard Mater 272, 75-82. Gong, S., Peng, Y., Jiang, P., Wang, M., Fan, M., Wang, X., Zhou, H., Li, H., 572 Yan, Q., Huang, T. et al. (2014). A deafness-associated tRNAHis mutation alters 573 the mitochondrial function, ROS production and membrane potential. Nucleic Acids 574 575 Res 42, 8039-48. 576 Houten, S. M. and Auwerx, J. (2004). PGC-1alpha: turbocharging

577 mitochondria. Cell 119, 5-7. Kim, H., Lee, Y. D., Kim, H. J., Lee, Z. H. and Kim, H. H. (2016). SOD2 and 578 579 Sirt3 Control Osteoclastogenesis by Regulating Mitochondrial ROS. J Bone Miner Res. 580 581 Lai, L., Yan, L., Gao, S., Hu, C. L., Ge, H., Davidow, A., Park, M., Bravo, C., Iwatsubo, K., Ishikawa, Y. et al. (2013). Type 5 adenylyl cyclase increases 582 583 oxidative stress by transcriptional regulation of manganese superoxide dismutase via the SIRT1/FoxO3a pathway. Circulation 127, 1692-701. 584 Li, W., Jue, T., Edwards, J., Wang, X. and Hintze, T. H. (2004). Changes in 585 586 NO bioavailability regulate cardiac O2 consumption: control by intramitochondrial 587 SOD2 and intracellular myoglobin. Am J Physiol Heart Circ Physiol 286, H47-54. 588 Mahaboob Basha, P. and Saumya, S. M. (2013). Suppression of mitochondrial 589 oxidative phosphorylation and TCA enzymes in discrete brain regions of mice 590 exposed to high fluoride: amelioration by Panax ginseng (Ginseng) and 591 Lagerstroemia speciosa (Banaba) extracts. Cell Mol Neurobiol 33, 453-64. 592 Miar, A., Hevia, D., Munoz-Cimadevilla, H., Astudillo, A., Velasco, J., Sainz, R. M. and Mayo, J. C. (2015). Manganese superoxide dismutase 593 594 (SOD2/MnSOD)/catalase and SOD2/GPx1 ratios as biomarkers for tumor 595 progression and metastasis in prostate, colon, and lung cancer. Free Radic Biol Med **85**, 45-55. 596 597 Millay, D. P. and Olson, E. N. (2013). Making muscle or mitochondria by selective splicing of PGC-1alpha. Cell Metab 17, 3-4. 598 Padmaja Divya, S., Pratheeshkumar, P., Son, Y. O., Vinod Roy, R., Andrew 599 600 Hitron, J., Kim, D., Dai, J., Wang, L., Asha, P., Huang, B. et al. (2015). Arsenic 601 Induces Insulin Resistance in Mouse Adipocytes and Myotubes Via Oxidative 602 Stress-Regulated Mitochondrial Sirt3-FOXO3a Signaling Pathway. Toxicol Sci 146, 603 290-300.

604 Park, S. J., Ahmad, F., Philp, A., Baar, K., Williams, T., Luo, H., Ke, H., 605 Rehmann, H., Taussig, R., Brown, A. L. et al. (2012). Resveratrol ameliorates aging-related metabolic phenotypes by inhibiting cAMP phosphodiesterases. Cell 606 607 **148**, 421-33. Pi, H., Xu, S., Reiter, R. J., Guo, P., Zhang, L., Li, Y., Li, M., Cao, Z., Tian, 608 609 L., Xie, J. et al. (2015). SIRT3-SOD2-mROS-dependent autophagy in 610 cadmium-induced hepatotoxicity and salvage by melatonin. Autophagy 11, 611 1037-51. Qiu, X., Brown, K., Hirschey, M. D., Verdin, E. and Chen, D. (2010). Calorie 612 restriction reduces oxidative stress by SIRT3-mediated SOD2 activation. Cell 613 614 *Metab* **12**, 662-7. 615 Ramis, M. R., Esteban, S., Miralles, A., Tan, D. X. and Reiter, R. J. (2015). 616 Protective Effects of Melatonin and Mitochondria-targeted Antioxidants Against 617 Oxidative Stress: A Review. Curr Med Chem 22, 2690-711. 618 San-Miguel, B., Crespo, I., Sanchez, D. I., Gonzalez-Fernandez, B., Ortiz de 619 Urbina, J. J., Tunon, M. J. and Gonzalez-Gallego, J. (2015). Melatonin inhibits autophagy and endoplasmic reticulum stress in mice with carbon 620 621 tetrachloride-induced fibrosis. J Pineal Res 59, 151-62. 622 Siu, A. W., Maldonado, M., Sanchez-Hidalgo, M., Tan, D. X. and Reiter, R. J. 623 (2006). Protective effects of melatonin in experimental free radical-related ocular diseases. J Pineal Res 40, 101-9. 624 Sundaresan, N. R., Gupta, M., Kim, G., Rajamohan, S. B., Isbatan, A. and 625 626 Gupta, M. P. (2009). Sirt3 blocks the cardiac hypertrophic response by augmenting 627 Foxo3a-dependent antioxidant defense mechanisms in mice. J Clin Invest 119, 2758-71. 628 629 Taghipour, N., Amini, H., Mosaferi, M., Yunesian, M., Pourakbar, M. and

Taghipour, H. (2016). National and sub-national drinking water fluoride

630

- concentrations and prevalence of fluorosis and of decayed, missed, and filled teeth
- in Iran from 1990 to 2015: a systematic review. Environ Sci Pollut Res Int 23,
- 633 5077-98.
- Tao, R., Coleman, M. C., Pennington, J. D., Ozden, O., Park, S. H., Jiang,
- 635 H., Kim, H. S., Flynn, C. R., Hill, S., Hayes McDonald, W. et al. (2010).
- 636 Sirt3-mediated deacetylation of evolutionarily conserved lysine 122 regulates
- 637 MnSOD activity in response to stress. *Mol Cell* **40**, 893-904.
- Tseng, A. H., Shieh, S. S. and Wang, D. L. (2013). SIRT3 deacetylates FOXO3
- to protect mitochondria against oxidative damage. Free Radic Biol Med 63, 222-34.
- Varol, E. and Varol, S. (2012). Effect of fluoride toxicity on cardiovascular
- systems: role of oxidative stress. *Arch Toxicol* **86**, 1627.
- Venegas, C., Garcia, J. A., Escames, G., Ortiz, F., Lopez, A., Doerrier, C.,
- 643 Garcia-Corzo, L., Lopez, L. C., Reiter, R. J. and Acuna-Castroviejo, D. (2012).
- Extrapineal melatonin: analysis of its subcellular distribution and daily fluctuations.
- 645 *J Pineal Res* **52**, 217-27.
- Wei, L., Zhou, Y., Qiao, C., Ni, T., Li, Z., You, Q., Guo, Q. and Lu, N. (2015).
- 647 Oroxylin A inhibits glycolysis-dependent proliferation of human breast cancer via
- promoting SIRT3-mediated SOD2 transcription and HIF1alpha destabilization. Cell
- 649 *Death Dis* **6**, e1714.
- 650 Wu, H., Wu, Y., Ai, Z., Yang, L., Gao, Y., Du, J., Guo, Z. and Zhang, Y.
- 651 (2014). Vitamin C enhances Nanog expression via activation of the JAK/STAT
- signaling pathway. Stem Cells 32, 166-76.
- 4653 Yan, X., Yang, X., Hao, X., Ren, Q., Gao, J., Wang, Y., Chang, N., Qiu, Y.
- and Song, G. (2015). Sodium Fluoride Induces Apoptosis in H9c2 Cardiomyocytes
- by Altering Mitochondrial Membrane Potential and Intracellular ROS Level. *Biol*
- 656 *Trace Elem Res* **166**, 210-5.
- 657 Ye, R., Kong, X., Yang, Q., Zhang, Y., Han, J. and Zhao, G. (2011).

Ginsenoside Rd attenuates redox imbalance and improves stroke outcome after focal cerebral ischemia in aged mice. *Neuropharmacology* **61**, 815-24. **Zhou, X., Chen, M., Zeng, X., Yang, J., Deng, H., Yi, L. and Mi, M. T.** (2014). Resveratrol regulates mitochondrial reactive oxygen species homeostasis through Sirt3 signaling pathway in human vascular endothelial cells. *Cell Death Dis* **5**, e1576. **Zhou, Y., Qiu, Y., He, J., Chen, X., Ding, Y., Wang, Y. and Liu, X.** (2013). The toxicity mechanism of sodium fluoride on fertility in female rats. *Food Chem Toxicol* **62**, 566-72.

00 101

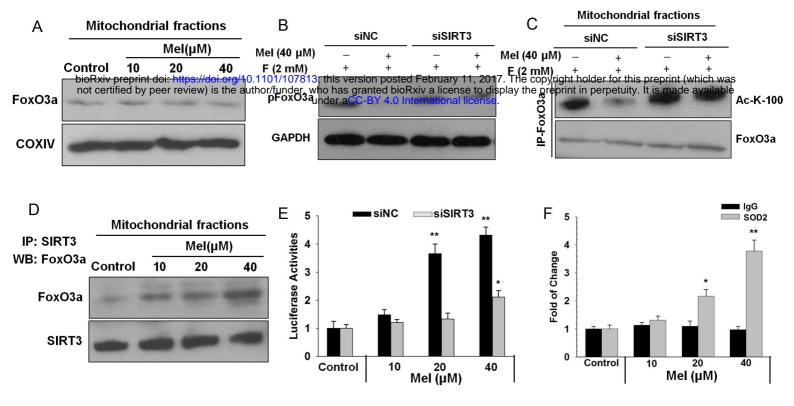
Annexin V-FITC

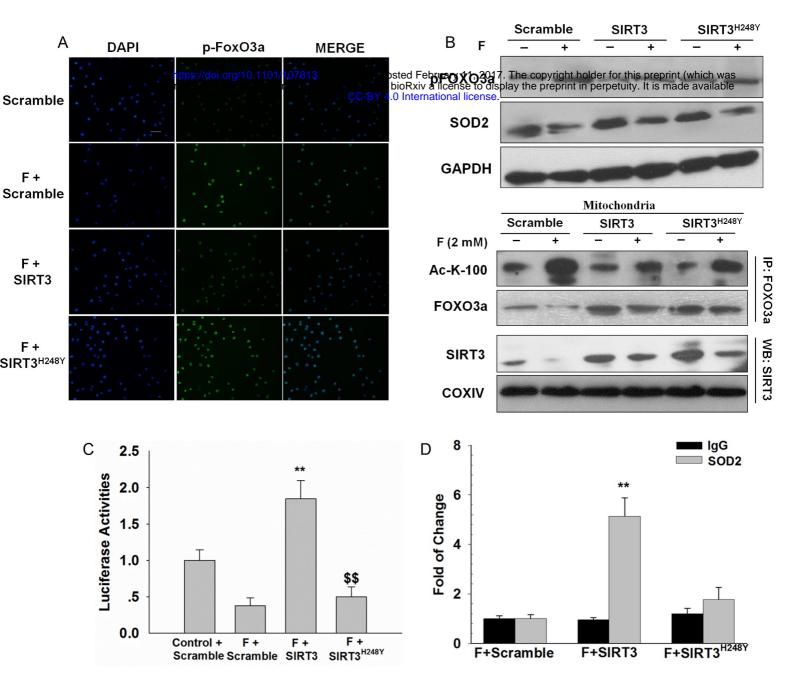
Annexin V-FITC

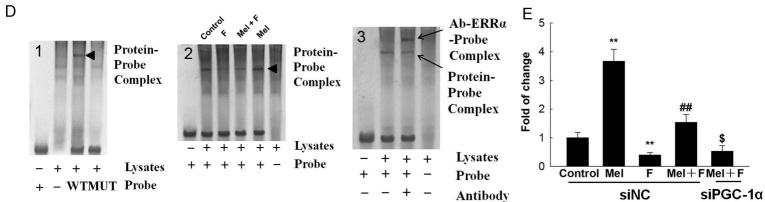
COXIV

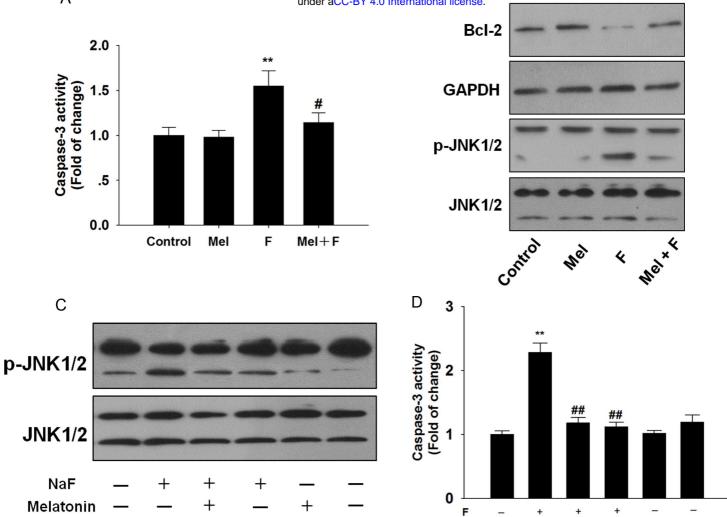
SiNC

SiSIRT3









SP600125

Mel

SP600125